Huang, C. (1969) *Biochemistry 8*, 344-351.
Huang, C., & Mason, J. T. (1978) *Proc. Natl. Acad. Sci. U.S.A. 75*, 308-310.
Johnson, S. M. (1973) *Biochim. Biophys. Acta 307*, 27-41.
Knauf, P. A. (1979) *Curr. Top. Membr. Transp. 12*, 249-363.
Nozaki, Y., & Tanford, C. (1967) *Methods Enzymol. 11*, 715-734.
Nozaki, Y., Reynolds, J. A., & Tanford, C. (1978) *Biochemistry 17*, 1239-1246.
Petri, W. A., & Wagner, R. R. (1979) *J. Biol. Chem. 254*, 4313-4316.
Racker, E., Violand, B., O'Neal, S., Alfonzo, M., & Telford, J. (1979) *Arch. Biochem. Biophys. 198*, 470-477.
Tanford, C., & Reynolds, J. A. (1976) *Biochim. Biophys. Acta 457*, 133-170.
Tosteson, M. T. (1978) *J. Membr. Biol. 38*, 291-309.
Tosteson, M. T., Lau, F., & Tosteson, D. C. (1973) *Nature (London), New Biol. 243*, 112-114.
Toyoshima, Y., & Thompson, T. E. (1975) *Biochemistry 14*, 1525-1531.
van Zoelen, E. J. J., de Kruijff, B., & van Deenen, L. L. M. (1978a) *Biochim. Biophys. Acta 508*, 97-108.
van Zoelen, E. J. J., van Dijck, P. W. M., de Kruijff, B., Verkleij, A. J., & van Deenen, L. L. M. (1978b) *Biochim. Biophys. Acta 514*, 9-24.

Lipid–Protein Interactions in Bacteriorhodopsin–Dimyristoylphosphatidylcholine Vesicles†

Maarten P. Heyn,* Richard J. Cherry, and Norbert A. Dencher

ABSTRACT: Bacteriorhodopsin (BR) was incorporated into large unilamellar dimyristoyl- and dipalmitoylphosphatidylcholine vesicles (100–300-nm radius). The effect of this intrinsic membrane protein on the order and dynamics of the lipids and on the cooperativity and transition temperature (T_c) of the gel to liquid-crystalline phase transition was investigated as a function of the lipid:protein ratio (L/BR). The lipid phase transition induces protein segregation. Above T_c, bacteriorhodopsin is in the monomeric state. Below T_c, BR is aggregated in the same hexagonal lattice as in the purple membrane (PM). In this reconstituted system, BR has a photochemical cycle similar to that in the PM and is active as a light-driven proton pump. The lipid phase transition which was monitored by using the steady-state anisotropy of the fluorescent probe 1,6-diphenyl-1,3,5-hexatriene (DPH) broadens with decreasing L/BR but occurs at approximately the same T_c. Below T_c, the fluorescence anisotropy of DPH is quite high (0.35) and independent of the L/BR. Above T_c, however, the anisotropy increases markedly with decreasing L/BR. It was recently pointed out that the fluorescence anisotropy of probes like DPH contains information not only on the dynamics (correlation times) but also on the order parameters of the lipids [Heyn, M. P. (1979) *FEBS Lett. 108*, 359–364]. The most likely explanation of the observed increase in anisotropy above T_c is that the perturbation of the lipid bilayer caused by the incorporation of BR leads both to an increase in order and to a slowing of the rotational diffusion of the lipids (increased viscosity). In agreement with this latter dynamical effect, the rotational diffusion constant of BR itself decreases above T_c with decreasing L/BR. Above T_c, the membrane viscosity as determined from the rotational diffusion constant of BR is at least 1.5 times larger than that obtained from the fluorescence depolarization of DPH. The formation of the BR lattice as a function of temperature was followed by using the circular dichroism (CD) exciton effect together with measurements of the rotational diffusion of BR. Both methods show similar transition curves for the protein crystallization whose midpoints, however, occur several degrees below T_c.

The study of lipid–protein interactions is of considerable importance in membrane biology. Such interactions affect the fluidity and order of the bilayer, modulate the enzymatic activity of membrane proteins, and are responsible for changes in the melting temperature and cooperativity of the gel to liquid-crystalline phase transition. Deuterium nuclear magnetic resonance (Seelig & Seelig, 1978; Oldfield et al., 1978), spin-labeling (Watts et al., 1979; Davoust et al., 1980), and Raman spectroscopy (Curatolo et al., 1978) have provided a detailed but as yet not consistent picture of the effect of intrinsic membrane proteins on lipid order. Much less is known about the perturbation caused by the incorporation of proteins on the dynamics of the lipid motion and on the rotation of the proteins themselves. Little is also known about the change in the thermodynamic parameters of the lipid-phase transition as a function of the lipid to protein ratio.

Reconstituted bacteriorhodopsin–phosphatidylcholine vesicles provide a well-characterized system for the study of lipid–protein interactions (Cherry et al., 1978; Dencher & Heyn, 1979). Bacteriorhodopsin (BR)[1] is an intrinsic membrane protein which spans the bilayer. Mixing of a suspension of solubilized monomeric BR with synthetic lipids above T_c

† From the Department of Biophysical Chemistry, Biocenter of the University of Basel, CH-4056 Basel, Switzerland (M.P.H., N.A.D.), and the Laboratorium für Biochemie, ETH, CH-8092 Zürich, Switzerland (R.J.C.). *Received June 3, 1980.* This work was supported by the Schweizerische Nationalfonds (Grants 3.333.78 and 3.570.79) and by the F. Hoffmann-La Roche Stiftung (Grant 160).

[1] Abbreviations used: CD, circular dichroism; L/BR, molar phospholipid to bacteriorhodopsin ratio; BR, bacteriorhodopsin; PM, purple membrane; DPH, 1,6-diphenyl-1,3,5-hexatriene; DMPC, dimyristoylphosphatidylcholine; DPPC, dipalmitoylphosphatidylcholine; T_c, midpoint temperature of the lipid gel to liquid-crystalline phase transition.

0006-2960/81/0420-0840$01.00/0

followed by detergent dialysis in the cold leads to large unilamellar vesicles which show lipid–protein segregation induced by the phase transition of the lipids. Below T_c the proteins are hexagonally crystallized; above T_c they are monomeric provided the L/BR is above ~40 (Cherry et al., 1978). Temperature-induced lateral segregation of lipids and proteins is a rather general phenomenon (Kleemann & McConnell, 1976; Höchli & Hackenbrock, 1976). In most of the recent studies on lipid–protein interactions, the state of aggregation of the proteins as a function of the temperature and the lipid:protein ratio was not determined. This lack of knowledge introduces considerable uncertainty into the conclusions of such studies. In most systems it is of course quite difficult to detect the presence of small protein aggregates. In the case of BR vesicles, the presence of such aggregates may be easily detected with the help of the exciton coupling effects in the CD spectra (Heyn et al., 1975). Another advantage of this system is that the lipid:protein ratio can be varied over a wide range (40–500 mol/mol). It is to be expected that the extent of the perturbation of the properties of the lipids will increase with decreasing lipid:protein ratio. Indeed, much may be learned from a systematic study of the dependency of various physical parameters on the lipid:protein ratio.

The turnover number of the photocycle of BR in these vesicles is about 7 times smaller than in the purple membrane, but the cycle is otherwise normal (Dencher & Heyn, 1979). It was recently shown that BR is active as a light-driven proton pump both above T_c (monomers) and below T_c (lattice) (Dencher & Heyn, 1979).

The purposes of the present study can be best summarized in the form of the following set of questions: (1) How does BR affect the temperature (T_c) and the cooperativity of the gel to liquid-crystalline phase transition of the lipids? (2) How does BR affect the order and dynamics of the bilayer lipids? (3) How does the lipid-phase transition affect the state of aggregation of the proteins? (4) How does the membrane viscosity as determined from the rotational diffusion of BR compare with that obtained from the rotational diffusion of a small probe in the lipid phase?

The first question was investigated by means of fluorescence depolarization measurements with the lipid-soluble probe DPH, which allow T_c and the van't Hoff enthalpy to be determined. T_c is not affected by the protein, but the cooperativity of the phase transition decreases. In a number of other lipid systems, the incorporation of proteins leads to considerable changes in T_c (Papahadjopoulos et al., 1975; Hartmann et al., 1978). The second question was also investigated with the help of fluorescence depolarization measurements with DPH since the fluorescence anisotropy of DPH contains information not only on membrane fluidity but also on the lipid order parameters (Heyn, 1979; Jähnig, 1979). Above T_c, the steady-state anisotropy increases markedly with decreasing lipid:protein ratio. The most likely explanation of this observation is that the perturbing effect of the protein on the lipids involves both an increase in their order parameter and an increase in their rotational correlation time. Regarding the third question, the lipid phase transition induces aggregation and crystallization of BR into a hexagonal lattice. These temperature-induced changes in the dynamical and structural properties of BR were investigated in two ways. The immobilization of BR which accompanies the formation of the crystalline-protein patch was monitored by the sharp decrease of its rotational diffusion constant near T_c. The formation of specific BR aggregates was also followed by the appearance of exciton bands in the visible CD spectrum, which are due to interactions between retinal chromophores of adjacent BR molecules. Both methods indicate that the protein crystallization occurs a few degrees below the lipid phase transition temperature. The fourth question was studied with separate labels in the two components of the system. The viscosity sensed by the small probe DPH was determined from its fluorescence depolarization. The viscosity as experienced by the large membrane protein BR was obtained from its diffusion constant for rotation around the normal to the bilayer. The latter viscosity is at least 1.5 times larger than the former. The theoretical framework to evaluate viscosities from rotational diffusion data is still in the stage of development for both methods. Nevertheless, it is worthwhile to see to what extent a consistent picture of membrane viscosity emerges.

Materials and Methods

Chemicals. Dimyristoylphosphatidylcholine (DMPC) and dipalmitoylphosphatidylcholine (DPPC) were obtained from Fluka. Since thin-layer chromatography showed only one spot, these lipids were used without further purification. 1,6-Diphenyl-1,3,5-hexatriene was obtained from Fluka. Triton X-100 and octyl β-D-glucoside were obtained from Packard and Calbiochem, respectively. Purple membranes (PM) were prepared from *Halobacterium halobium* R_1 M_1 according to standard procedures (Oesterhelt & Stoeckenius, 1974; Bauer et al., 1976). This material showed a single band in Na-$DodSO_4$–polyacrylamide gel electrophoresis. Protein concentrations were determined by the method of Lowry et al. (1951). The results were corrected for a systematic error in the case of BR (Rehorek & Heyn, 1979). Phospholipid concentrations were determined by phosphorus analysis (Ames & Dubin, 1960).

Preparation of Phosphatidylcholine–Bacteriorhodopsin Vesicles. BR was solubilized to the state of monomers in either Triton X-100 or octyl β-D-glucoside (Dencher & Heyn, 1978, 1980). In this procedure, the endogenous lipids (about ten per bacteriorhodopsin) are not removed. The monomeric BR was mixed with DMPC or DPPC at the required lipid:protein ratio. During prolonged detergent dialysis, unilamellar vesicles are formed which are purified by sucrose density centrifugation (Cherry et al., 1978). More details concerning the dialysis procedure and the properties of the reconstituted vesicles can be found elsewhere (Heyn & Dencher, 1980). After dialysis the vesicles contain about one Triton X-100 molecule per two bacteriorhodopsins (Cherry et al., 1978). The reconstituted vesicles were examined in the electron microscope by negative staining and were found to be predominantly unilamellar, with radii varying between 100 and 300 nm (Cherry et al., 1978). Similar values for the average radius were obtained from quasi-elastic light scattering. The latter measurements showed that the mean radius is almost independent of the lipid:protein ratio and that the size distribution is narrowest for vesicles with the lowest lipid to protein ratios. For DMPC vesicles, one sharp purple band is observed in the sucrose gradient. The photochemical cycle of BR in DMPC vesicles is an order of magnitude slower than in the purple membrane (Dencher & Heyn, 1979). Upon illumination, protons are pumped inward, and an alkalization of the medium occurs both above and below the T_c of the lipids (Dencher & Heyn, 1979). This shows that the reconstituted vesicles are functional and have a net protein orientation. Bleached vesicles were prepared by reacting with hydroxylamine at pH 5 in the light. Unless otherwise stated, all experiments were performed in 0.1 M sodium acetate buffer, pH 5.0.

CD Measurements. CD measurements were performed with a Cary 61 spectropolarimeter modified with a 18-kHz mod-

ulator (Bächinger et al., 1979). The transition from monomeric to aggregated BR as a function of temperature was followed by measuring the ellipticity at a fixed wavelength (590 nm) in thermostated cylindrical cells from Helma. The temperature was measured with a thermistor inside the cell. The CD signal and the temperature were recorded on a dual channel recorder as a function of time while the cell was slowly heated at a rate of 12 or 18 °C/h. The linear heating scans (usually from 5 to 50 °C) were controlled by a Lauda control unit.

BR Rotational Diffusion Measurements. Rotational diffusion of bacteriorhodopsin in the lipid vesicles was measured by observing flash-induced transient dichroism. Details of the experimental method are given elsewhere (Cherry, 1978). Briefly, the sample is excited by a linearly polarized light pulse of 1–2-μs duration and 540-nm wavelength. Transient absorbance changes due to ground-state depletion are detected at 568 nm. The signals are analyzed by calculating the absorption anisotropy $r(t)$ given by

$$r(t) = \frac{A_{\parallel}(t) - A_{\perp}(t)}{A_{\parallel}(t) + 2A_{\perp}(t)} \quad (1)$$

where $A_{\parallel}(t)$ and $A_{\perp}(t)$ are the absorbance changes at time t after the flash for light polarized parallel and perpendicular with respect to the polarization of the exciting light. The results reported here were obtained by storing and averaging the signals from 16 or 32 flashes with a Datalab DL 102A signal averager. Data analysis was accomplished by a Hewlett–Packard HP 9825 A desk-top computer interfaced to the signal averager. The rotational diffusion coefficient $D_{\parallel}$ for rotation of BR around an axis normal to the bilayer can be obtained from an analysis of the time dependence of the absorption anisotropy $r(t)$ at 568 nm on the basis of (Heyn et al., 1977a; Cherry et al., 1976):

$$r(t) = A_1 e^{-D_{\parallel}t} + A_2 e^{-4D_{\parallel}t} + A_3 \quad (2)$$

The coefficients A_1, A_2, and A_3 are functions of the angle θ between the 568-nm transition dipole moment and the normal to the bilayer. Recent studies demonstrate that eq 2 provides a good fit to the experimental $r(t)$ above the T_c when the L/Br is greater than about 100, indicating the existence of a single rotating species (R. E. Godfrey and R. J. Cherry, unpublished results). The best fit is obtained with $\theta \sim 78°$ [corresponding to a ratio $A_3/(A_1 + A_2 + A_3)$ of 0.19], in agreement with earlier studies (Heyn et al., 1977a). Below T_c, data analysis indicates the existence of multiple populations, presumably corresponding to aggregated and nonaggregated BR. Here we have fitted the $r(t)$ curves above and below T_c to eq 2 using an iterative nonlinear least-squares program in which A_1, A_2, and A_3 are variable and the ratio $A_3/(A_1 + A_2 + A_3)$ is constrained to the value 0.19. Below T_c, this procedure provides an estimate of the average $D_{\parallel}$ of different BR populations. At the highest temperatures, the values of $D_{\parallel}$ are rather inaccurate because the rotational relaxation time $\phi_{\parallel} = D_{\parallel}^{-1}$ becomes quite short and approaches the limit of resolution of the apparatus (5 μs). Finally, below 12.5 °C, the data could no longer be fitted to eq 2. This is at least in part due to the fact that at low temperatures the rotational diffusion constant of the whole vesicles (radius ranging from 0.1 to 0.3 μm) in aqueous solution becomes comparable to that of BR in the hydrophobic core of the bilayer. In this low temperature range (far below T_c), the data were instead fitted to the simpler equation

$$r(t) = A_1 e^{-D_{\parallel}t} + A_3 \quad (3)$$

with the constraint $A_1/(A_1 + A_3) = 0.19$.

In previous experiments with similar vesicles, the initial anisotropy $r(0)$ was considerably below the theoretically expected upper limit of 0.4 (Cherry et al., 1977, 1978; Heyn et al., 1977a). In a recent report, this difference was attributed to fast wobbling of the chromophore (Jähnig, 1979). This conclusion is incorrect, however. The reduced value of $r(0)$ is mainly due to the high laser intensity. The theoretical limit of 0.4 is only reached when a negligible fraction of the chromophores is excited. At lower light intensities and by use of signal averaging, a higher value of 0.37 was determined. It is to be expected that upon extrapolation to zero intensity and with highly diluted vesicles (depolarization due to light scattering) the theoretical limit of 0.4 is approached. The ratio $r(0)/r(\infty)$ was unaffected by changes in the laser intensity.

Steady-State Fluorescence Depolarization Experiments. DPH stock solutions were prepared in tetrahydrofuran. The label was incorporated in the vesicles by incubation for 30 min far above T_c (Shinitzky & Barenholz, 1978). DPH: phospholipid ratios were usually 1:900 (mol/mol). Fluorescence depolarization measurements were carried out with a Schoeffel RRS 1000 recording fluorimeter. The excitation beam was polarized by a Glan–Thompson polarizer. The emitted light was analyzed with Polacoat sheet polarizers. Excitation was at 360 nm, and emission was measured at 428 nm. The steady-state fluorescence anisotropy $\bar{r}$ is defined by

$$\bar{r} = \frac{I_{\parallel} - I_{\perp}}{I_{\parallel} + 2I_{\perp}} \quad (4)$$

where $I_{\parallel}$ and $I_{\perp}$ are the two fluorescence intensities with the analyzer parallel and perpendicular, respectively, to the vertical polarizer. Standard corrections for depolarization in the detection system were made (Azumi & McGlynn, 1962). The effect of depolarization due to light scattering was tested (Lentz et al., 1979). Dilution over a 50-fold range had no effect on the measured anisotropy values. The turbidity of the vesicle suspensions was rather small. The lipid concentrations were typically of the order of 0.25 mg/mL. DPH in glycerin at −15 °C was used to test the performance of our apparatus. Anisotropy values of 0.39 were obtained. In order to achieve such high values, stops were used to limit the solid angles of the diverging beams. Increasing the label: phospholipid ratio to 1:100 had no significant effect on the $\bar{r}$ vs. temperature curve. The vesicle suspensions were contained in 1 × 0.4 cm stoppered fluorescence cuvettes. The temperature was measured by a thermistor immersed in the suspension above the light beam. Below 10 °C, the sample compartment was flushed with nitrogen to prevent condensation. The temperature was increased automatically at a rate of 12 or 18 °C/h as described under CD measurements. The two fluorescence intensities, $I_{\parallel}$ and $I_{\perp}$, were alternately recorded by rotating the analyzer over 90°. The two fluorescence intensities and the temperature were recorded as a function of time on a dual channel recorder. These data were then converted into $\bar{r}$ vs. T curves. Some of the data were also collected in a T geometry with two photomultipliers measuring $I_{\parallel}$ and $I_{\perp}$ simultaneously. The two measuring channels were balanced, with the polarizer in the horizontal position. The two fluorescence intensities were, in this case, converted electronically to anisotropy values, and the transition curves of $\bar{r}$ vs. temperature were directly available on an X-Y recorder. Some irreversible loss of fluorescence intensity occurred during a heating run, as is usually the case when DPH is irradiated (Shinitzky & Barenholz, 1978). The anisotropy depends, however, only on the ratio of the two fluorescence intensities.

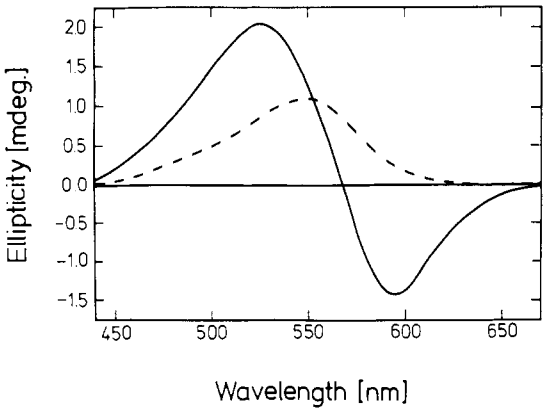

FIGURE 1: Change in the CD spectrum of a suspension of bacteriorhodopsin–DMPC vesicles when the temperature is raised from 0.6 (—) to 35.0 °C (– – –). Molar phospholipid:bacteriorhodopsin ratio 117. The vesicles were suspended in 0.1 M sodium acetate (pH 5.0).

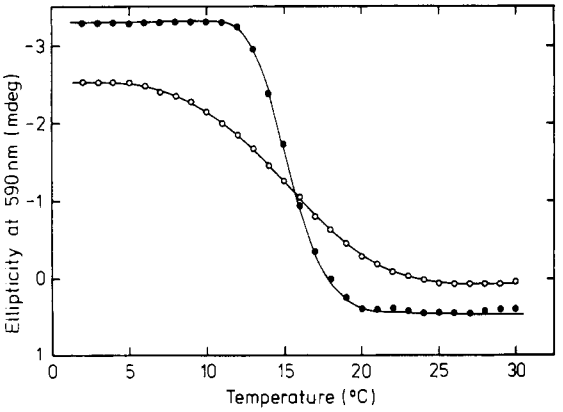

FIGURE 2: Formation of the protein lattice in BR–DMPC vesicles as monitored by the temperature dependence of the BR circular dichroism at 590 nm. At high temperatures, BR is in the monomeric state; at low temperatures BR is aggregated (see Figure 1). The transition is reversible. (●) DMPC:BR ratio 135; (○) DMPC:BR ratio 71.

The change in $\bar{r}$ with temperature was completely reversible.

Results and Analysis

Circular Dichroism. Figure 1 shows the change in the CD spectrum of BR–DMPC vesicles when the temperature is raised from 0.6 °C to 35.0 °C, i.e., from below the lipid phase transition to above. The low-temperature spectrum has the pair of positive and negative exciton bands characteristic of the hexagonally aggregated state of bacteriorhodopsin. The high-temperature spectrum consists of a broad positive band typical for monomeric BR (Dencher & Heyn, 1978). In previous work, it was shown that these features of the CD spectrum can be used to monitor the state of aggregation of BR (Heyn et al., 1975; Bauer et al., 1976; Heyn et al., 1977b; Cherry et al., 1978b). Note that the quality of the vesicle CD spectrum of Figure 1 is much better than previously reported (Cherry et al., 1978). This is due to the fact that the present experiments were performed with clear vesicle suspensions which scatter light only to a minor extent whereas the previous spectra were obtained with turbid suspensions and were consequently distorted. The difference between the CD spectra of monomeric and aggregated BR is maximal at about 590 nm. Transition curves between these two states as a function of temperature were therefore determined at this wavelength. Figure 2 shows the change in ellipticity at 590 nm as a function of temperature for DMPC–BR vesicles of two phospholipid:protein ratios. Below 11 °C and above 23 °C, the CD signal reaches plateau values indicating that the transition

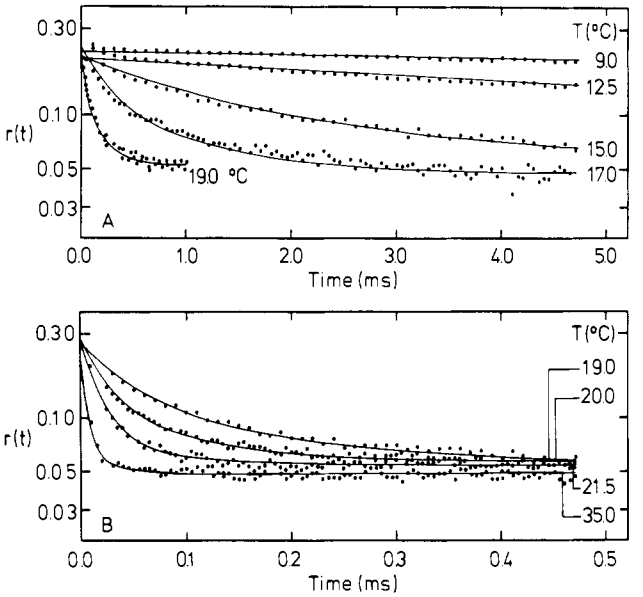

FIGURE 3: Time dependence of the absorption anisotropy r of 568-nm depletion signals from BR–DMPC vesicles at various temperatures. Molar phospholipid:protein ratio 111. The vesicles were suspended in 0.1 M sodium acetate (pH 5.0). The solid lines were obtained by fitting the experimental points to eq 2 above 12.5 °C and to eq 3 at 12.5 °C and below. At fixed time, $r(t)$ decreases monotonically with increasing temperature. (A) Decay of r for temperatures from 9.0 to 19.0 °C. (B) Decay of r for temperatures from 19.0 to 35.0 °C. Note that in (A) the time scale is 10 times longer than in (B).

between monomeric and aggregated BR is completed. In our previous work, it was shown that in the aggregated state of BR at low temperatures, the BR molecules are arranged in the same hexagonal lattice as in the PM (Cherry et al., 1978). We can therefore characterize the transition as monitored by the CD as a protein crystallization. From Figure 2, we note that with decreasing lipid to protein ratio the transition seems to broaden. After normalization of the curves, however, this effect is much less pronounced. The midpoint temperature of the transition is independent of the lipid:protein ratio. The transition is halfway over at about 17 °C, which is well below the phase-transition temperature of the lipids (23.5 °C). At the latter temperature, the BR molecules are still in the monomeric form according to Figure 2. Experiments performed with DPPC–BR vesicles (T_c of 41 °C) show that the crystallization is shifted downward by several degrees in that case as well. The transition of Figure 2 is reversible and shows no hysteresis. Further reduction of the temperature scanning rate had no effect.

Rotational Diffusion. Figure 3 shows the data of the flash-induced transient linear dichroism experiments. The data are plotted as absorption anisotropy r vs. time. The continuous curves represent least-squares fits according to eq 2 or 3. It is apparent from this figure that with increasing temperature the initial decay of r becomes faster, corresponding to an increase in the rotational diffusion constant $D_{\parallel}$. Typically, the rotational relaxation time $\phi_{\parallel} = D_{\parallel}^{-1}$ changes from about 15 μs well above T_c to about 30 ms well below T_c. For each temperature, $D_{\parallel}$ was determined as described under Materials and Methods. Figure 4 shows the diffusion constant $D_{\parallel}$ for rotation of BR around an axis perpendicular to the bilayer as a function of the temperature at two phospholipid to protein ratios. As the temperature is lowered from 25 to 12 °C, the diffusion constant decreases by more than 3 orders of magnitude, in agreement with the expected immobilization of BR in the protein lattice. At the lipid:protein ratio of 168, the transition is slightly steeper than at the ratio of 111. Above

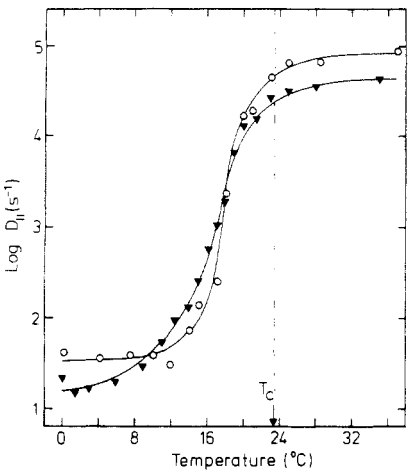

FIGURE 4: Temperature dependence of the diffusion constant $D_{\parallel}$ for rotation of BR around an axis normal to the vesicle bilayer. $D_{\parallel}$ is obtained by fitting the experimental points (Figure 3) to eq 2 or eq 3. (▼) L/BR = 111. (○) L/BR = 168. The data for the L/BR of 111 were fitted to eq 3 for temperatures less than or equal to 12.5 °C and to eq 2 for temperatures above 12.5 °C. The data for the L/BR of 168 were fitted to eq 3 for temperatures less than or equal to 15 °C and to eq 2 for temperatures above 15 °C. The arrow labeled with T_c at 23.5 °C indicates the position of the midpoint of the lipid-phase transition (see Figure 5). The vesicles were suspended in 0.1 M sodium acetate (pH 5.0).

25 °C where according to the CD results BR is monomeric, the value of $D_{\parallel}$ is highest for the higher lipid:protein ratio. This is consistent with the results of earlier experiments with the same vesicle system (Cherry et al., 1977), which showed that above T_c the rotational diffusion constant increases with increasing lipid:protein ratio (in the range where BR is monomeric). The protein aggregation transition as monitored by the immobilization of the rotational motion of BR also clearly occurs below the lipid phase transition temperature of 23.5 °C. Since complete immobilization corresponds to $D_{\parallel} = 0$, no plateau should be observed in the log $D_{\parallel}$ vs. T plot of Figure 4 at the low-temperature end of the transition. The occurrence of this plateau is due to the fact that at low temperatures the rotation of BR within the hydrophobic core of the viscous bilayer becomes slower than the rotation of the vesicles in the aqueous solution. If BR is indeed completely immobilized upon lowering of the temperature, vesicle tumbling will eventually dominate, no matter how large the vesicles are. It is not possible to subtract out the contribution from the slowly tumbling vesicles. This would require knowledge of the distribution of the vesicle radii and a determination of the end values of the $r(t)$ curves at the lower temperatures. Because of this low-temperature leveling off of the log $D_{\parallel}$ vs. T curve, the midpoint of the transition has no precise significance. Nevertheless for a comparison with the CD results, an approximate midpoint can be determined. From the logarithmic plot of Figure 4, the midpoint appears to occur close to 17.5 °C. A linear presentation of the data leads to a somewhat higher value. However, no matter how the midpoint of the protein transition is determined, it occurs as in the case of the CD measurements below T_c. The transition shown in Figure 4 is reversible.

Steady-State Fluorescence Depolarization. Figure 5 shows the steady-state fluorescence anisotropy of DPH embedded in DMPC–BR vesicles of various lipid:protein ratios as a function of the temperature. For the protein-free vesicles, the lipid-phase transition as monitored by the fluorescence anisotropy of DPH occurs at 23.5 °C, as expected. With decreasing lipid:protein ratio, the transition broadens, but its midpoint appears to remain close to 23 °C. The transition

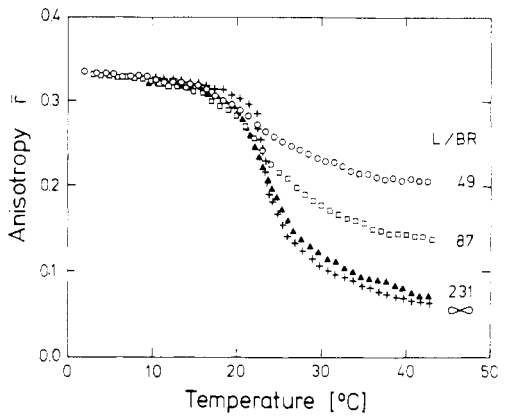

FIGURE 5: Temperature dependence of the fluorescence anisotropy $\bar{r}$ of DPH incorporated in unilamellar BR–DMPC vesicles of various phospholipid:protein ratios. The molar phospholipid:bacteriorhodopsin ratios (L/BR) are indicated on the right-hand side. The steepest transition is observed with protein-free vesicles (+). The molar DMPC:DPH ratio was about 1000. The vesicles were suspended in 0.1 M sodium acetate (pH 5.0).

curves in Figure 5 were treated more quantitatively in the following way. First, end values were determined by linear extrapolation of the high-temperature data to lower temperatures and of the low-temperature data to higher temperatures. At any given temperature, we can then calculate the difference between $\bar{r}(T)$ and the lower end value and the difference between the two end values. The degree of transition $\theta(T)$ is now defined in the usual way as the ratio of these two numbers. In this way, normalized transition curves were obtained with the degree of transition ranging between 1 (far below the phase transition) and 0 (at very high temperatures). The transition midpoints corresponding to the lipid-phase transition temperature occur at $\theta = 1/2$. They decrease for the four samples of Figure 5 from 23.3 °C at a L/BR of ∞ to 22.2 °C at a L/BR ratio of 49. When the assumption is made that the gel to liquid-crystalline transition as monitored by the DPH fluorescence can be considered in a first approximation to be a two-state equilibrium, the association constant K can be determined from $\theta(T)$. In that case, $K = \theta/(1-\theta)$ and the van't Hoff enthalpy $\Delta H_{\text{van't Hoff}}$ can be obtained either from a plot of log K vs. $1/T$ or from the slope of the transition curve at $\theta = 1/2$ [$\Delta H_{\text{van't Hoff}} = 4RT_c^2(\partial\theta/\partial T)_{T_c}$].

For the four curves of Figure 5 with the lipid to protein ratios of 49, 87, 231, and ∞, we obtain in this way $\Delta H_{\text{van't Hoff}}$ values of −56.1, −65.3, −89.5 and −209.5 kcal/mol, respectively. These numbers show that the lipid-phase transition becomes steeper and more cooperative when the amount of protein is reduced. The most interesting aspect of Figure 5 is the fact that the $\bar{r}$ values far below the transition temperature when the lipids are crystalline are practically independent of the lipid:protein ratio whereas the $\bar{r}$ values far above T_c when the proteins are monomeric strongly increase when the protein content is increased. The interpretation of this observation will be discussed below. Conversion of retinal into retinal oxime by reaction with hydroxylamine in the light leads to an increase in fluorescence but does not affect the anisotropy $\bar{r}$. The change in anisotropy with temperature is reversible.

Discussion

Effect of Incorporated Bacteriorhodopsin on the Temperature and Cooperativity of the Gel to Liquid-Crystalline Phase Transition of the Lipids. The fluorescence depolarization experiments with DPH show that the temperature of the transition is almost unaffected when BR is incorporated into

DMPC vesicles. A slight decrease in T_c was observed with decreasing L/BR (from 23.3 °C to 22.2 °C), but this change is not much larger than the experimental error in the determination of T_c. The steepness of the transition curves decreases markedly when more and more BR is incorporated, as one would expect. This steepness could be quantified in terms of a van't Hoff enthalpy for the transition which decreases with decreasing L/BR. The van't Hoff enthalpy obtained from the fluorescence depolarization of DPH agrees well with that determined from differential scanning calorimetry on the same vesicles (A. Blume, N. A. Dencher, M. P. Heyn, and M. Rehorek, unpublished results). This shows that it appears to be possible to obtain reliable thermodynamic parameters for the lipid-phase transition from fluorescence depolarization measurements with an embedded label. The cooperativity of the transition, defined as the ratio of the van't Hoff and the calorimetric enthalpy, also decreases with decreasing L/BR (A. Blume, N. A. Dencher, M. P. Heyn, and M. Rehorek, unpublished results).

Effect of the Transmembrane Protein Bacteriorhodopsin on the Order Parameter and Dynamics of the Bilayer Lipids. It has recently been shown that the time-resolved fluorescence anisotropy of DPH in pure lipid systems (Kawato et al., 1977; Kinosita et al., 1977; Chen et al., 1977; Dale et al., 1977; Lakowicz et al., 1979) and in lipid bilayers containing cholesterol (Kawato et al., 1978; Lakowicz et al., 1979; Veatch & Stryer, 1977) or proteins (Glatz, 1978; Senê et al., 1978; Hildenbrand & Nicolau, 1979) can be described phenomenologically in the following way:

$$r_F(t) = r_\infty + (r_0 - r_\infty)e^{-t/\tau_c} \tag{5}$$

The fluorescence anisotropy $r_F(t)$ decays exponentially with correlation time τ_c from an initial value r_0 to a constant residual anisotropy r_∞. The parameter r_∞ describes the fact that the rotational diffusion of the label is restricted and that its equilibrium orientational distribution is anisotropic. When $r_\infty = 0$, the equilibrium distribution reached at long times after the flash is isotropic. r_∞ is a measure of the order parameter of the label, which in turn reflects the order parameter of the lipids in its neighborhood. It can indeed be shown that for a stiff rod-like molecule like DPH with absorption and emission transition dipole moments parallel to the long axis, the following relationship holds between the order parameter S and the end value r_∞ (Heyn, 1979; Jähnig, 1979; Kinosita et al., 1977):

$$\frac{r_\infty}{r_0} = S^2 \tag{6}$$

The order parameter S is defined in the customary way in terms of the angle θ between the long axis of DPH and the membrane normal and in terms of the orientational distribution function $f(\theta)$:

$$S = \int_{-1}^{+1} \left(\frac{3\cos^2\theta - 1}{2} \right) f(\theta)\, \mathrm{d}\cos\theta \tag{7}$$

Recently, an encouraging correlation was found between the order parameter of the lipids as determined by deuterium magnetic resonance and the order parameter of DPH embedded in these lipids as determined from its fluorescence depolarization according to eq 6 (Heyn, 1979; Jähnig, 1979). Further details concerning this correlation and the relationship between r_∞/r_0 and the order parameter can be found elsewhere (Heyn, 1979).

τ_c is the correlation time for the approach to the anisotropic equilibrium distribution. It characterizes the dynamics of the restricted rotational motion and is proportional to the viscosity experienced by the probe.

Equation 5 describes the decay of $r_F(t)$ in response to a delta-function excitation by linearly polarized light at time zero. Steady-state fluorescence depolarization experiments are more common and easier to perform. The expression corresponding to eq 5 for the steady-state fluorescence anisotropy $\bar{r}$ can be easily obtained by integration of eq 5 after multiplication with the fluorescence decay function (characterized by the fluorescence lifetime τ_F):

$$\bar{r} = r_\infty + (r_0 - r_\infty)\frac{\tau_c}{\tau_c + \tau_F} \tag{8}$$

It is apparent from eq 8 that in contrast to the case of time-dependent measurements the information on the order and on the dynamics is no longer separable in steady-state experiments. In general, neither r_∞ nor τ_c can be determined from a measurement of $\bar{r}$. Setting $r_\infty = 0$ in eq 8 leads to the familiar Perrin equation. Note that eqs 5 and 8 provide only a lowest order description of $r_F(t)$ and $\bar{r}$, respectively. The simplifying assumption was made of a single fluorescence lifetime and a single correlation time. If we represent the rodlike molecule DPH as an ellipsoid, two rotational correlation times are expected. Rotation around the long axis of the ellipsoid does not lead to significant depolarization, however, since both the absorption and the emission dipole moments are almost parallel to this axis. Only the wobbling motion around an axis perpendicular to the long axis leads to depolarization, and the assumption of a single wobbling rotational correlation time τ_c seems to be a good approximation. We will discuss our results on the basis of eq 8.

Below the lipid phase transition, the steady-state anisotropy $\bar{r}$ is independent of the lipid:protein ratio and attains very high values (about 0.34) corresponding to almost completely immobilized DPH (Figure 5). This constancy may be explained in two ways. We recall that below T_c the BR molecules are segregated and form a hexagonal protein lattice for all lipid:protein ratios. If the DPH stays in the lipid phase when the protein patch is formed, it will always be in the same crystalline lipid environment and have the same $\bar{r}$. Alternatively, DPH may distribute equally between various membrane regions as has been claimed (Moore et al., 1978). We find for DPH embedded in purple membrane $\bar{r}$ values ranging from 0.35 at 6 °C to 0.32 at 66 °C. This is considerably higher than the previously reported values of 0.29 at 4 °C and 0.21 at 71.5 °C (Korenstein et al., 1976). Since the BR patches below T_c have the same hexagonal lattice structure as in the PM, it is reasonable to assume that $\bar{r}$ for DPH in these patches has approximately the same high value. In the range of molar lipid:protein ratios used (38–390), the main contribution to $\bar{r}$ will come from the bulk crystalline lipid phase. Since the relative contribution from DPH trapped in the protein patch is small and since $\bar{r}$ for those DPH's is not much different from those in the crystalline-lipid phase, we expect negligible variation of $\bar{r}$ with the lipid:protein ratio.

Above T_c, we observe a marked increase in $\bar{r}$ with decreasing L/BR. On the basis of eq 8, this effect could be due to an increase in r_∞, to an increase in τ_c, or to a reduction in τ_F with decreasing L/BR. We will now discuss these three possibilities, which may of course also occur in combination, separately.

From eq 8 we note that $\bar{r}$ is a function of the ratio of τ_c and τ_F. This is intuitively clear since the depolarization must depend on the rotational diffusion which can take place within the fluorescence lifetime. The dependence of $\bar{r}$ on τ_F and τ_c can therefore be best discussed together. In Figure 6, the

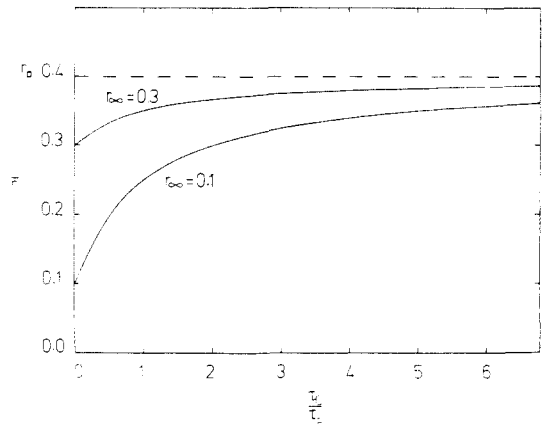

FIGURE 6: Dependence of the steady-state anisotropy $\bar{r}$ on the ratio of the rotational correlation time τ_c and the fluorescence lifetime τ_F. The curves were calculated according to eq 8. For the lower curve, $r_\infty = 0.1$; for the upper curve, $r_\infty = 0.3$. r_0 was assumed to be 0.4. $\bar{r}$ is approximately equal to r_∞ only when τ_c/τ_F is close to zero. The difference $(\bar{r} - r_\infty)$ is largest when r_∞ is small.

dependence of $\bar{r}$ on the ratio τ_c/τ_F is plotted for two values of r_∞. When $\tau_c/\tau_F \ll 1$, the label rotation is fast on the fluorescence time scale, and r_∞ is reached. When $\tau_c/\tau_F \gg 1$, the label is essentially frozen on the fluorescence time scale and $\bar{r} = r_0$. These two extreme values are connected according to eq 8 by a simple hyperbola. It is clear from Figure 6 that an increase in τ_c has the same effect on $\bar{r}$ as a decrease in τ_F. We will now discuss these two possible ways of increasing τ_c/τ_F separately.

The fluorescence lifetime τ_F may decrease because of energy transfer from DPH to the bacteriorhodopsin-bound retinal. The lifetime would then be expected to decrease gradually with increasing surface density of bacteriorhodopsin (decreasing L/BR). Energy transfer between the donor DPH and the acceptor retinal has been observed for rod outer segment disk membranes which contain the visual pigment rhodopsin (Stubbs et al., 1976). The probability of energy transfer depends critically on the overlap integral between the donor (DPH) emission spectrum and the acceptor (bound retinal) absorption spectrum. The absorption of retinal in bacteriorhodopsin has its maximum at 568 nm, i.e., is shifted approximately 70 nm to the red with respect to rhodopsin. The spectral overlap and with it the distance R_0 between donor and acceptor at which energy transfer is equally probable with all other decay processes of the excited state are therefore much less than in the case of rhodopsin since the orientational factor K^2 is also about the same in the two cases. For effective energy transfer to occur, the distance between donor and acceptor must be of the order of R_0 or less. The molar phospholipid:rhodopsin ratio in rod outer segment disk membranes is estimated to be about 75, i.e., lower than the L/BR in most of our samples. The protein surface density is thus lower than in the rhodopsin system, leading to larger mean donor–acceptor distances. In accordance with these considerations, we observed only a small increase in DPH fluorescence when the acceptor was converted into retinal oxime (absorbing at 360 nm), indicating that the amount of energy transfer is small. Moreover, this change in the acceptor absorption spectrum had no effect on $\bar{r}$. Preliminary nanosecond fluorescence measurements show that the lifetime of DPH in vesicles containing BR is somewhat shorter than in vesicles without BR (M. Rehorek, N. A. Dencher, and M. P. Heyn, unpublished results).

From Figure 6 we see than an increase in τ_c with decreasing L/BR may also explain the observed increase in $\bar{r}$. This means that in the presence of the large incorporated protein molecules the rotational diffusion of the label is slowed down, corresponding to an increase in the effective membrane viscosity. Indeed, as will be discussed in more detail below, such an effect of the L/BR on BR's own rotational relaxation time $D_{\parallel}^{-1}$ has been observed with these vesicles. In another system, a rise in the protein concentration led to a decrease in the translational diffusion constant of the lipids (Wu et al., 1978) which is also consistent with an increased viscosity. For pure DMPC or DPPC vesicles, τ_c is about 1 ns (Kawato et al., 1977; Chen et al., 1977; Lakowicz et al., 1979). The few available measurements on the decay of $r_F(t)$ for DPH embedded in protein-containing membranes indicate that τ_c is indeed larger and ranges between 2 and 4 ns (Glatz, 1978; Senê et al., 1978; Hildenbrand & Nicolau, 1979). It thus seems likely that the presence of proteins increases τ_c. It is, therefore, reasonable to assume that in this system, too, τ_c of DPH increases with decreasing L/BR. This assumption is also consistent with parallel observations on the effect of L/BR on the rotational correlation time of BR (see below). Let us assume that for our BR–DMPC vesicles τ_c increases to 4 ns at the lowest L/BR. We may then calculate the expected increase in $\bar{r}$ on the basis of eq 8 or read it off from Figure 6. Other numbers which enter the calculation are τ_F [~10 ns; Shinitsky & Barenholz (1978)] and r_0 [0.39; Kawato et al. (1979); our observations]. The ratio τ_c/τ_F thus increases from about 0.1 in the absence of bacteriorhodopsin to a maximum value of 0.4 in its presence. From Figure 6 we see that even at the low value of 0.1 for r_∞ (above T_c) the expected increase in $\bar{r}$ on the basis of this effect is too small to explain the experimental results of Figure 5. One is thus forced to conclude that besides the increase in τ_c also an increase in r_∞ occurs. According to eq 8 this means that incorporation of BR also leads to an increase in lipid order. Time-resolved fluorescence depolarization experiments in which r_∞ and τ_c can be determined separately are required to confirm this explanation.

In a recent paper on Ca-ATPase–DMPC vesicles, a similar increase in $\bar{r}$ with decreasing lipid:protein ratio was observed above T_c (Gomêz-Fernández et al., 1979). These authors concluded that this effect was due to an increase in microviscosity, i.e., to a decrease in the rate of rotational diffusion. The effect was thus ascribed entirely to an increase in τ_c. Our discussion shows that quite possibly the major effect is due to an increase in r_∞ (order) and that in general both effects have to be considered. A number of authors have already pointed out that the steady-state anisotropy $\bar{r}$ is always considerably larger in protein-containing membranes than in the extracted lipids (Moore et al., 1978; Fraley et al., 1978; Stubbs et al., 1976). The interpretation of these results in terms of an increase in microviscosity has been unsatisfactory, however. Equation 8 provides the basis for a more comprehensive interpretation and shows that in the absence of energy transfer an increase in $\bar{r}$ can be due to an increase in microviscosity (effect on the rate of motion, on the dynamics), to an increased restriction in the label rotation (steric effect, order), or to a combination of the two.

In conclusion, we may say that the perturbation of the lipids caused by the incorporation of the transmembrane protein BR leads both to an increase in the lipid order and to an increase in the viscosity.

Effect of the Lipid Phase Transition on the Aggregation of Bacteriorhodopsin. From our previous work, we know that BR is hexagonally crystallized far below T_c and monomeric above T_c [at lipid:protein ratios (mol/mol) above ~40)]. Both the CD and the rotational diffusion measurements indicate

that the BR crystallization occurs several degrees below the midpoint of the lipid phase transtion for both DMPC and DPPC vesicles. The midpoint for the CD transitions is between 16 and 17 °C, somewhat lower than the midpoint of the transition in $D_{\parallel}(T)$. There is no need for agreement among these two methods concerning this midpoint since the various BR aggregates are weighted in a different manner in the two methods. Whereas all specific BR aggregates starting from dimers and trimers have exciton CD spectra of similar amplitude and splitting, the rotational diffusion constant of BR aggregates decreases with the inverse square of the aggregate radius and thus varies widely from dimers to larger aggregates. Several interpretations of the observed effect are possible. When the BR molecules are cooled through the lipid phase transition, they may prefer to stay in the remaining fluid lipid phase in which they become highly concentrated. In these segregated protein-rich patches, the viscosity is expected to be quite high, and some decrease of $D_{\parallel}$ will already occur. The CD, on the other hand, will remain that of monomers since no specific aggregates are formed. BR crystallization would take place only at the end of the lipid-phase transition when no fluid lipid is left. On the basis of this primitive model, the protein transition would be shifted to lower temperatures by about the width of the lipid-phase transition (several degrees). In this model, one expects a slight decrease in T_c with decreasing L/BR, as is actually observed.

Alternatively, the depression of the protein crystallization below T_c may be explained by a slight modification of a recent theory on protein–protein interactions (Schroeder, 1977). In this theory, the attractive interaction between two proteins contains a correlation length which is maximal at the phase transition temperature. At T_c, the range of the interaction is maximal, but the attractive force is small. The interaction is most effective at a slightly smaller correlation length, which occurs both above and below T_c. The state of lowest energy is achieved a few degrees below T_c (H. Schroeder, private communication). Near T_c, critical fluctuations may indeed play a role, and it is conceivable that the fluctuations in order which lead below T_c to disorder and which increase in amplitude when T_c is approached occur predominantly near BR. The protein may in a sense attract these fluctuations, bringing it in a fluid environment below T_c (F. Jähnig, private communication). To what extent this phenomenon is of more general significance is at present unclear. A similar effect has recently been observed. The large decrease in the translational diffusion constant of gramicidin S incorporated in DMPC bilayers occurred at a temperature which was lower than the DMPC melting temperature as determined by differential scanning calorimetry (Wu et al., 1978). The formation of protein aggregates which are induced by the lipid-phase transition has also been discussed from the point of view of packing faults (Chapman et al., 1977).

Comparison of the Membrane Viscosity As Determined from the Rotational Diffusion Constant of BR with That Obtained from the Rotational Diffusion of DPH. There is no a priori reason why the membrane viscosity as sensed by the small rodlike molecule DPH should be the same as that observed by the large protein BR with its highly irregular surface structure. Considerations based on continuum theories are expected to be more appropriate for the rotational motion of BR than for that of DPH. Whereas DPH may make rapid wobbling motions of small amplitude, BR will drag along lipid molecules in its rotational motion. Nevertheless, since the microviscosity concept is used so frequently, a comparison is of considerable interest.

The magnitude of the diffusion constant $D_{\parallel}$ for the rotation of BR around the normal to the membrane may be discussed on the basis of eq 9 (Saffman & Delbrück, 1975):

$$D_{\parallel} = \frac{kT}{4\pi a^2 h \eta} \tag{9}$$

T is the absolute temperature, k is Boltzmann's constant, and η is the membrane viscosity. In this theory, the protein is idealized by a cylinder of radius a embedded in the bilayer to the depth h. Rotation occurs around the cylinder axis which coincides with the membrane normal. This theory has not yet been critically tested. The currently available data on $D_{\parallel}$ and on the size of membrane proteins are consistent with eq 9 if one assumes membrane viscosities between 1 and 10 P (Cherry, 1979). On the basis of the electron microscopically determined dimensions of BR monomers in the PM of 25 × 35 × 45 Å^3 (Henderson & Unwin, 1975), we calculate a = 16.7 Å and h = 45 Å. Since BR is functional as a light-driven proton pump in these vesicles (Dencher & Heyn, 1979) and therefore spans the membrane, it is reasonable to use the same numbers for the reconstituted vesicles. With the help of eq 9, it is thus possible to interpret the measured values for $D_{\parallel}$ in terms of a membrane viscosity η as reported by BR if we assume that the rotating particle is a monomer. Note that according to eq 9 η depends in a very sensitive way on the choice of the radius of the rotating cylinders. Using eq 9, we calculate that at 25 °C η = 8.6 P at a L/BR of 111[2] and 3.5 P at a L/BR of 168. At 25 °C, the CD transition is over (see Figure 2), and we may indeed assume BR to be mainly monomeric. In a recent abstract, a value of 2.1 ± 1.1 P was reported for BR–DMPC vesicles of a L/BR of 193 at 26 °C (Wey et al., 1979). This value is directly comparable to ours since both the method of vesicle preparation and the method for the determination of the viscosity from $D_{\parallel}$ were the same as described here. In their calculation, a and h equalled 18 and 35 Å, respectively, and it was assumed that BR was monomeric. In view of the decrease in η with increasing L/BR, the value of 2.1 P appears to be in good agreement with our results.

It is also possible to calculate a so-called "microviscosity" from the steady-state fluorescence anisotropy of DPH by using the standard procedure (Shinitzky & Barenholz, 1978). For the same two samples mentioned above, we find at 25 °C a viscosity of 2.9 P at the L/BR of 111 and of 2.3 P at the L/BR of 168. We note that the same trend seems to be present as in the viscosities obtained from the rotation of BR: the sample with the highest relative protein content had the highest viscosity. It is of interest to compare these values with those obtained with DPH in bovine rod outer segment disk membranes which contain the related protein rhodopsin. In these membranes, which do not show a phase transition and which have a phospholipid:rhodopsin ratio of 68, a microviscosity of 3.8 P was determined at 20 °C (Stubbs et al., 1976). Our present results are in general agreement with this result on disk membranes, in particular, if one takes the dependence of the viscosity on the lipid:protein ratio into account.

In the procedure for the calculation of the microviscosity, it is assumed that $r_\infty = 0$ (Shinitzky & Barenholz, 1978). It is intuitively clear that setting r_∞ equal to zero in a case of restricted rotation leads to too high values for the microvis-

[2] However, very recent investigations involving curve fitting of the anisotropy decay data indicate that a small proportion of aggregates may be present at 25 °C in the L/BR = 111 samples (R. J. Cherry and R. E. Godfrey, unpublished results). This would tend to increase the apparent viscosity obtained as described above so that the actual viscosity may be somewhat lower.

cosity. Since $\bar{r}$ is the integral of the product of $r(t)$ and the fluorescence decay function, the correlation time τ_c has to be smaller in the case of $r_\infty \neq 0$ than in the case of $r_\infty = 0$. This follows also immediately from the inverted version of eq 8:

$$\tau_c = \tau_F(\bar{r} - r_\infty)/(r_0 - \bar{r}) \quad (10)$$

τ_c is proportional to the viscosity η, but the proportionality constant depends in the case of restricted rotation also on r_∞ (Kinosita et al., 1977). To a first approximation, the correct viscosity ($\eta_{r_\infty \neq 0}$) is related to the viscosity obtained under the assumption $r_\infty = 0$ ($\eta_{r_\infty = 0}$) in the following way:

$$\eta_{r_\infty \neq 0} = \left(\frac{\bar{r} - r_\infty}{r_0 - r_\infty}\right)\frac{r_0}{\bar{r}}\,\eta_{r_\infty = 0} \quad (11)$$

Since $r_\infty < \bar{r} < r_0$, it is clear that $\eta_{r_\infty \neq 0}$ is always smaller than $\eta_{r_\infty = 0}$. Setting $r_\infty = 0$ thus leads to an overestimate of η, and the present values of 2.9 and 2.3 P therefore represent upper bounds for the viscosity. From eq 11 we see that the neglect of r_∞ will be particularly serious when r_∞ is large, i.e., at low L/BR ratios. In this connection, we note that indeed the discrepancy between the viscosities obtained from the rotational diffusion of BR and the fluorescence depolarization of DPH appears larger at the L/BR ratio of 111 than at 168. In view of the fact that the correct values for the microviscosity are likely to be smaller than those calculated above, it is probable that the viscosity values obtained from the BR rotation are larger than those obtained from the DPH rotation. A more detailed comparison between the apparent viscosities obtained by these two methods is feasible when τ_c and r_∞ are determined directly from time-dependent fluorescence depolarization measurements.

References

Ames, B. N., & Dubin, D. T. (1960) *J. Biol. Chem. 235*, 769–775.

Azumi, T., & McGlynn, S. P. (1962) *J. Chem. Phys. 37*, 2413–2420.

Bächinger, H. P., Eggenberger, H. P., & Hänisch, G. (1979) *Rev. Sci. Instrum. 50*, 1367–1372.

Bauer, P.-J., Dencher, N. A., & Heyn, M. P. (1976) *Biophys. Struct. Mech. 2*, 79–92.

Chapman, D., Cornell, B. A., & Quinn, P. J. (1977) in *Biochemistry of Membrane Transport* (Semenza, G., & Carafoli, E., Eds.) pp 72–85, Springer-Verlag, West Berlin.

Chen, L. A., Dale, R. E., Roth, S., & Brand, L. (1977) *J. Biol. Chem. 252*, 2163–2169.

Cherry, R. J. (1978) *Methods Enzymol. 54*, 47–61.

Cherry, R. J., Bürkli, A., Busslinger, M., Schneider, G., & Parish, G. R. (1976) *Nature (London) 263*, 389–393.

Cherry, R. J., Müller, U., & Schneider, G. (1977) *FEBS Lett. 80*, 465–469.

Cherry, R. J., Müller, U., Henderson, R., & Heyn, M. P. (1978) *J. Mol. Biol. 121*, 283–298.

Curatolo, W., Verma, S. P., Sakura, J. D., Small, D. M., Shipley, G. G., & Wallach, D. F. H. (1978) *Biochemistry 17*, 1802–1807.

Dale, R. E., Chen, L. A., & Brand, L. (1977) *J. Biol. Chem. 252*, 7500–7510.

Davoust, J., Bienvenue, A., Fellmann, P., & Devaux, P. F. (1980) *Biochim. Biophys. Acta 596*, 28–42.

Dencher, N. A., & Heyn, M. P. (1978) *FEBS Lett. 96*, 322–326.

Dencher, N. A., & Heyn, M. P. (1979) *FEBS Lett. 108*, 307–310.

Dencher, N. A., & Heyn, M. P. (1980) *Methods Enzymol.* (in press).

Fraley, R. T., Jameson, D. M., & Kaplan, S. (1978) *Biochim. Biophys. Acta 511*, 52–69.

Glatz, P. (1978) *Anal. Biochem. 87*, 187–194.

Gômez-Fernández, J. C., Goñi, F. M., Bach, D., Restall, C., & Chapman, D. (1979) *FEBS Lett. 98*, 224–228.

Hartmann, W., Galla, H.-J., & Sackmann, E. (1978) *Biochim. Biophys. Acta 510*, 124–139.

Henderson, R., & Unwin, P. N. T. (1975) *Nature (London) 257*, 28–32.

Heyn, M. P. (1979) *FEBS Lett. 108*, 359–364.

Heyn, M. P., & Dencher, N. A. (1980) *Methods Enzymol.* (in press).

Heyn, M. P., Bauer, P.-J., & Dencher, N. A. (1975) *Biochem. Biophys. Res. Commun. 67*, 897–903.

Heyn, M. P., Cherry, R. J., & Müller, U. (1977a) *J. Mol. Biol. 117*, 607–620.

Heyn, M. P., Bauer, P.-J., & Dencher, N. A. (1977b) in *Biochemistry of Membrane Transport* (Semenza, G., & Carafoli, E., Eds.) pp 96–104, Springer-Verlag, West Berlin.

Hildenbrand, K., & Nicolau, C. (1979) *Biochim. Biophys. Acta 553*, 365–377.

Höchli, M., & Hackenbrock, C. R. (1976) *Proc. Natl. Acad. Sci. U.S.A. 73*, 1636–1640.

Jähnig, F. (1979) *Proc. Natl. Acad. Sci. U.S.A. 76*, 6361–6365.

Kawato, S., Kinosita, K., Jr., & Ikegami, A. (1977) *Biochemistry 16*, 2319–2324.

Kawato, S., Kinosita, K., Jr., & Ikegami, A. (1978) *Biochemistry 17*, 5026–5031.

Kinosita, K., Jr., Kawato, S., & Ikegami, A. (1977) *Biophys. J. 20*, 289–305.

Kleemann, W., & McConnell, H. M. (1976) *Biochim. Biophys. Acta 419*, 206–222.

Korenstein, R., Sherman, W. V., & Caplan, S. R. (1976) *Biophys. Struct. Mech. 2*, 267–276.

Lakowicz, J. R., Prendergast, F. G., & Hogen, D. (1979) *Biochemistry 18*, 508–519.

Lentz, B. R., Moore, B. M., & Barrow, D. A. (1979) *Biophys. J. 25*, 489–494.

Lowry, O. H., Rosebrough, N. J., Farr, A. L., & Randall, R. J. (1951) *J. Biol. Chem. 193*, 265–275.

Moore, B. M., Lentz, B. R., & Meissner, G. (1978) *Biochemistry 17*, 5248–5255.

Oesterhelt, D., & Stoeckenius, W. (1974) *Methods Enzymol. 31*, 667–678.

Oldfield, E., Gilmore, R., Glaser, M., Gutowsky, H. S., Hshung, J. C., Kang, S. Y., King, T. E., Meadows, M., & Rice, D. (1978) *Proc. Natl. Acad. Sci. U.S.A. 75*, 4657–4660.

Papahadjopoulos, D., Moscarello, M., Eylar, E. H., & Isac, T. (1975) *Biochim. Biophys. Acta 401*, 317–335.

Rehorek, M., & Heyn, M. P. (1979) *Biochemistry 18*, 4977–4983.

Saffman, P. G., & Delbrück, M. (1975) *Proc. Natl. Acad. Sci. U.S.A. 72*, 3111–3113.

Schroeder, H. (1977) *J. Chem. Phys. 67*, 1617–1619.

Seelig, A., & Seelig, J. (1978) *Hoppe-Seyler's Z. Physiol. Chem. 359*, 1747–1756.

Senē, C., Genest, D., Obrēnovitch, A., Wahl, P., & Monsigny, M. (1978) *FEBS Lett. 88*, 181–186.

Shinitzky, M., & Barenholz, Y. (1978) *Biochim. Biophys. Acta 515*, 367–394.

Stubbs, G. W., Litman, B. J., & Barenholz, Y. (1976) *Biochemistry 15*, 2766–2772.

Veatch, W. R., & Stryer, L. (1977) *J. Mol. Biol. 117*, 1109–1113.
Watts, A., Volotovski, I. D., & Marsh, D. (1979) *Biochemistry 18*, 5006–5013.
Wey, C. L., Ahl, P. L., Cone, R. A., & Gaffney, B. J. (1979) *Biophys. J. 25*, 169a.
Wu, E.-S., Jacobson, K., Szoka, F., & Portis, A., Jr. (1978) *Biochemistry 17*, 5543–5550.

Affinities of Amino Acid Side Chains for Solvent Water†

R. Wolfenden,* L. Andersson, P. M. Cullis, and C. C. B. Southgate

ABSTRACT: Equilibria of distribution of amino acid side chains, between their dilute aqueous solutions and the vapor phase at 25 °C, have been determined by dynamic vapor pressure measurements. After correction to pH 7, the resulting scale of "hydration potentials", or free energies of transfer from the vapor phase to neutral aqueous solution, spans a range of ~22 kcal/mol. The side chain of arginine is much more hydrophilic than those of the other common amino acids, with an equilibrium constant of $\sim 10^{15}$ for transfer from the vapor phase to neutral aqueous solution. Hydration potentials are more closely correlated with the relative tendencies of the various amino acids to appear at the surface of globular proteins than had been evident from earlier distribution studies on the free amino acids. Both properties are associated with a pronounced bias in the genetic code.

In biological systems, "chemical recognition" usually depends on the structural complementarity of different compounds or functional groups that are attracted to each other by noncovalent forces. When these interactions occur in an aqueous environment, solvent water must usually be stripped away from the interacting groups. If information were available about the absolute tendencies of these compounds to leave water and enter an empty cavity that neither attracts nor repeals solutes, then it might be possible to draw inferences about specific forces of attraction or repulsion that may be at work in specific cases.

The absolute affinity of a compound for an aqueous environment can be evaluated by determining its vapor pressure over dilute aqueous solutions. From the results, it is a simple matter to calculate a dimensionless equilibrium constant for its transfer from water to a featureless "solvent" of unit dielectric constant, the dilute vapor phase. Measurements of this kind, performed on a variety of organic compounds, suggest that the free energy of interaction between complex molecules and water can usually be approximated as an additive function of their constituent groups (Butler, 1937; Hine & Mookerjee, 1975). Earlier measurements were confined to relatively volatile solutes that exhibit substantial vapor pressures over water. More sensitive techniques have allowed the recent extension of these measurements to include polar molecules bearing functional groups of biological interest such as the peptide bond (Wolfenden, 1976, 1978).

Differences between amino acid residues, in their strength of solvation by water, are likely to be significant in determining the configurations of proteins in solution (Kauzmann, 1959; Tanford, 1962; Perutz, 1965). It would therefore be of interest to have information about the relative affinities of amino acid side chains for solvent water. Even using material of very high specific activity, efforts in this laboratory to detect glycine in the vapor phase over concentrated aqueous solutions have been unavailing. This is hardly surprising, since glycine in neutral aqueous solution is present as the uncharged species only to the extent of ~1 part in 200 000 (Edsall & Wyman, 1958). Free energies of solvation of charged ammonium and carboxylate groups are each in the neighborhood of −70 to −80 kcal/mol [Kebarle, 1976; see also Tse et al. (1978)], so that the zwitterionic species of glycine in water can be considered totally nonvolatile. The rare, uncharged species of glycine can be expected, from bond contributions based on correlations of data from the literature (Hine & Moorkerjee, 1975), to exhibit an equilibrium constant of $\sim 8 \times 10^{-10}$ for transfer from dilute aqueous solution to the vapor phase. Accordingly, the concentration of glycine, at equilibrium in the vapor phase over an aqueous solution containing 1 M glycine, is expected to be no higher than 10^{-14} M; much lower values are expected for more polar amino acids.

Even if methods more sensitive than those presently available should make it possible in the future to determine free energies for removal of amino acids from water to the vapor phase, it is far from clear that they would serve as good models (even in a relative sense) for the behavior of the various amino acid residues in proteins. It has even been suggested that there may be no significant relationship between free energies of transfer of amino acids from water to organic solvents and their tendencies to appear in internal peptide linkage in the interior rather than at the surface of globular proteins (Janin, 1979). This would seem to indicate either that solvation effects may be less important than originally suspected or that free amino acids are poor models for the relative solvation behavior of amino acids in proteins. Side chains of amino acids in proteins are flanked by peptide bonds, associated with a free energy of solvation of about −10 kcal/mol (Wolfenden, 1978), modest in comparison with the large negative free energies of solvation of ammonium and carboxylate groups mentioned above. The solvent-organizing power of these charged groups is very great and might be expected to affect the relative distribution properties of nearby substituents (Nemethy, 1967; Nandi, 1976).

To obtain results that might be more closely comparable with the solvation behavior expected of amino acids in polypeptides, we decided to examine the behavior of the amino acid

† From the Department of Biochemistry, University of North Carolina, Chapel Hill, North Carolina 27514. *Received June 17, 1980.* Supported by grants from the National Science Foundation (PCM-7823016) and the National Institutes of Health (GM-18325) and by fellowships from the American-Scandinavian Foundation (to L.A.) and from the Jane Coffin Childs Foundation (to P.M.C.).

0006-2960/81/0420-0849$01.00/0